THE JOURNAL OF PHYSICAL CHEMISTRY Letters

ACS Editors' Choice

Letter

pubs.acs.org/JPCL

Kinetically Controlled Self-Assembly of Latex–Microgel Core–Satellite Particles

Mario Tagliazucchi, Fengwei Zou, and Emily A. Weiss*

Department of Chemistry, Northwestern University, Evanston, Illinois 60208-3113, United States

Supporting Information

ABSTRACT: Latex–microgel core–satellite particles were prepared by electrostatic assembly of negatively charged polystyrene latex and positively charged microgels of a poly(*N*-isopropylmethacrylamide) (pNIPMAM) and poly[2-methacryloyloxy)ethyl] trimethylammonium chloride (pMETAC) copolymer. The number of satellites per core, determined by scanning electron microscopy, varied from 3 to 10 depending on the sizes of the microgel and latex microparticles. The numbers of satellites per core for different size ratios were compared with the predictions for thermodynamically controlled (maximum packing) and kinetically controlled (random sequential adsorption) assembly, and it was shown that the assembly of latex and microgel proceeds through a random sequential adsorption mechanism. The charges of the microgels and latex particles were retained within the assemblies; therefore, the core–satellite particles have well-defined regions of positive and negative charge. These regions were used to direct the adsorption of gold and latex nanoparticles of opposite charge in order to create multicomponent colloids.

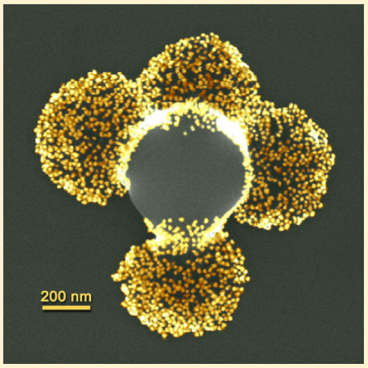

SECTION: Glasses, Colloids, Polymers, and Soft Matter

This Letter describes the mechanism of electrostatic assembly of core–satellite particles, where the cores are polystyrene latex microparticles and the satellites are microgels of poly(*N*-isopropylmethacrylamide) (pNIPMAM) and poly[2-methacryloyloxy)ethyl] trimethylammonium chloride (pMETAC) copolymer. We show that the number of microgel satellites per latex core can be controlled by the ratio of the diameters of the two types of particles, in good agreement with the predictions of the random sequential adsorption (RSA) model. The microgels and latex particles retain their charges in the assemblies, such that we can subsequently assemble smaller nanoparticles (NPs) onto one or the other component to form hierarchical colloidal clusters. Patches of chemical functionality or electrostatic charge within assemblies of nano and microparticles[1−3] allow colloids to interact anisotropically with other particles or surfaces in order to form extended ("colloidal crystals")[3] or nonextended ("colloidal molecules")[4−6] structures. Control over the stoichiometry of colloidal assemblies comprising two or more different types of particles enables fundamental studies of charge and energy transfer[7] and electrodynamic coupling[8−11] between NPs. Moreover, patchy and core–satellite particles are useful in fabricating films with hierarchical roughness for superhydrophobic and superhydrophilic substrates.[12,13]

In previous studies, core–satellite particles have been assembled using electrostatic forces,[11,14] depletion interactions,[15] liquid coalescence,[16] DNA hybridization,[7,17] hydrogen bonding,[18] covalent bonds,[12] and metal–ligand interactions.[19] Electrostatic interactions are especially appealing due to their ubiquitous nature, ability to direct equilibrium[20] and out-of-equilibrium[21] self-assembly and control by pH and ionic strength. Previous electrostatically self-assembled core–satellite and core–shell colloids used satellite particles much smaller than the core particle (with some exceptions[11,14,22]); this self-assembly process resulted in homogeneous coating of the central particle. In contrast to this previous work, we focus here on the limit where the sizes of the central particle and the satellites are similar and, therefore, each colloidal assembly has between 3 and 10 satellites per central particle. The satellites are soft thermoresponsive microgels of a pNIPMAM/pMETAC copolymer. These microgels have a water content of 85–95%, and shrink to 35–50% of their initial size upon drying to create spaced microgel patches on the surface of the core particles (see Figure 1a and b). The formation of well-spaced patches by microgels was documented on planar substrates[23−25] and large spheres[26] (which adsorb tens of microgels per particle) but not on particles of similar size. Moreover, none of the studies that addressed the interactions between microgels and particles with similar size and opposite charge[27−32] reported well-defined core–satellite structures like those that we obtain here. We also show that the core–satellite particles have well-defined positively and negatively charged regions, which we use to direct the assembly of smaller gold particles onto each component of the core–satellite colloids (Figure 1c–f).

Received: July 1, 2014
Accepted: July 28, 2014
Published: July 28, 2014

   dx.doi.org/10.1021/jz5013609 | *J. Phys. Chem. Lett.* 2014, 5, 2775–2780

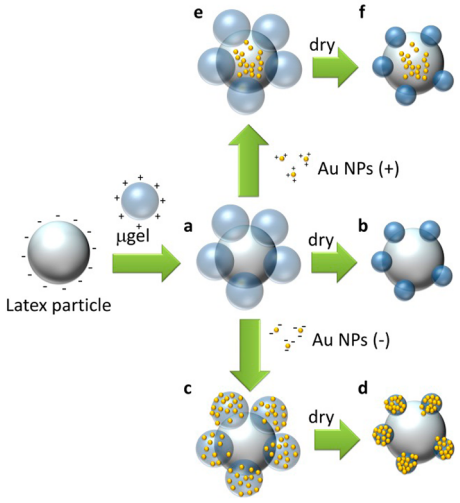

Figure 1. Scheme showing the electrostatic self-assembly of core–satellite NPs. In the first step, positively charged microgel particles adsorb on latex particles in order to produce latex–microgel core–satellite particles (a). Drying of the sample collapses the microgel particles to 35–50% of their initial size (b). Negatively (c) or positively (e) charged Au NPs added to the latex–microgels core–satellite particles attach to the microgel satellites or the latex core, respectively, and produce hierarchical assemblies (d,f).

We investigated the assembly of carboxylate-coated polystyrene latex particles, which have negative charge at pH = 8 (all solutions were adjusted to this pH), and pNIPMAM/pMETAC microgels, which have pH-independent positive charges due to the quaternary ammonium groups in the pMETAC structure. We studied the aggregation behavior of mixtures of these two types of particles by mixing them in different ratios, drying a few drops of the resulting solution on a flat silicon substrate, and imaging this sample with a scanning electron microscope (SEM). Table 1 compiles the properties of the different latex particles and microgels used in these experiments. The mixtures of microgels and latex particles yielded stable dispersions when the ratio of microgels to latex particles was larger than a threshold value (which depends on the size of both particles); below this threshold value, the particles precipitated within a few minutes. For example, a mixture of the 690 nm microgels and 510 or 300 nm latex microparticles produced stable solutions for microgel/latex ratios larger than 7 and 4, respectively. Scanning electron microscopy revealed that these dispersions contained core–satellite assemblies comprising a central latex particle surrounded by microgel satellites. Figure 2 shows images of latex–microgel core–satellite colloids for different combinations of particle sizes. It is important to remember that upon drying, the microgels shrink to ~35–50% of their size in solution; therefore, while the microgels are sparse on the surface of the latex particle in the SEM images, they are more densely packed before drying. Interestingly, the number of satellites surrounding the central latex particle is on the same order of magnitude as the threshold ratio required for colloidal stability. For example, mixtures of 690 nm microgels with 510 and 300 nm latex particles have threshold microgel/latex ratios of 7 and 4 and an average number of microgels per latex of 4.5 ± 0.5 and 2.9 ± 0.4.

In addition to core–satellite particles, our dried samples contained isolated microgels (that did not adsorb to any latex particles) and aggregates with more than one latex particle. We imaged random regions of the drop-casted samples in order to quantify the fraction of latex particles that form isolated core–satellite particles and the fraction that form larger aggregates (see Figure S1 in the Supporting Information). The fraction of latex particles that form the desired core–satellite assemblies depends critically on the microgel/latex ratio. For a large excess of microgels over latex particles (microgel:latex ratio = 70:1 for a mixture of 690 nm microgels and 510 nm latex), 77% of the 144 latex particles observed formed isolated core–satellite assemblies, and the remaining particles formed small aggregates containing two or three latex particles per aggregate. In the aggregates, the latex particles were bridged by microgels. In contrast, for a microgel/latex ratio of 21, we found that only 5% of the 900 latex microparticles observed formed isolated core–satellite colloids, while the rest formed large aggregates with two or more latex particles. These large aggregates were disordered networks of latex particles bridged by microgels. The average number of microgel satellites around the latex central particle (determined only for isolated core–satellite particles) was independent of the microgel/latex ratio; we counted 4.7 ± 0.7 and 4.5 ± 0.5 microgels per latex particle for

Table 1. Properties of the Colloids Used in this Study

colloid	charged groups	diameter/nm	z potential/mV	charges per particle	area per charge (nm^2)
latex 300 nm	carboxylates	300 ± 10[a]	−32	1.7 × 10^5[e]	1.62
latex 600 nm	carboxylates	590 ± 10[a]	−36	2.0 × 10^6[e]	0.55
latex 800 nm	carboxylates	780 ± 20[a]	−44	9.5 × 10^5[e]	2.11
latex 510 nm	carboxylates	510 ± 10[a]	−64	1.4 × 10^5–2.3 × 10^5[e]	0.35–0.59
microgels 690 nm	quaternary ammonium	332 ± 55 (dry)[a] 690 ± 90 (swollen)[b] 740 ± 27 (swollen)[c]	15	5.1 × 10^5[f]	0.34
microgels 600 nm	quaternary ammonium	211 ± 21 (dry)[a] 600 ± 100 (swollen)[b] 635 ± 12 (swollen)[c]	7	2.6 × 10^5[f]	0.45
Au NPs	carboxylates	32 ± 4[d]	−10	–	–
Au NPs coated with PDDA	carboxylates/quaternary ammonium	32 ± 4[d]	12	–	–
negative latex np	carboxylates	60[e]	−70	3 × 10^3[f]	3.7

[a]Size determined from SEM. [b]Size determined from two-dimensional close-packed structures. [c]Size determined from DLS. [d]Size determined from TEM. [e]According to manufacturer specifications. [f]Charge determined from the dry size and ratio of the monomers used in the synthesis.

dx.doi.org/10.1021/jz5013609 | J. Phys. Chem. Lett. 2014, 5, 2775–2780

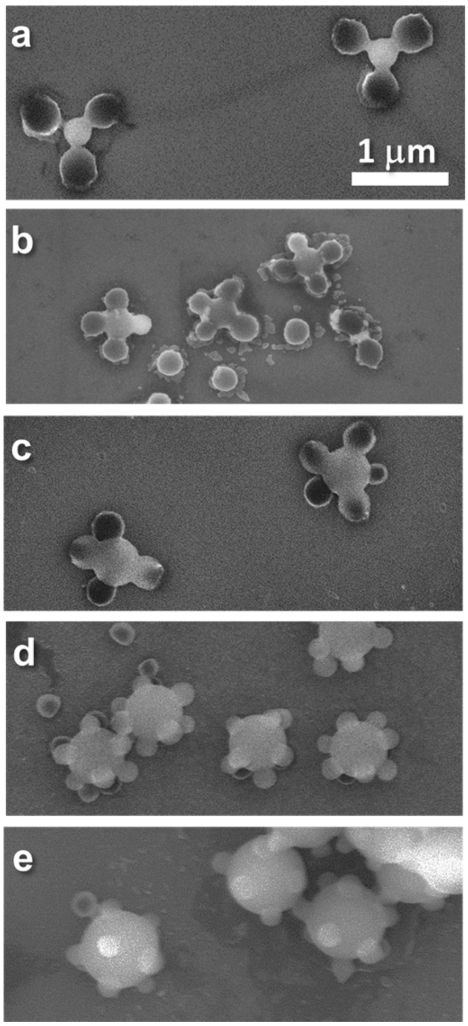

Figure 2. Examples of latex−microgel core−satellite particles for different combinations of sizes. The sizes of the microgels (in solution)/latex particles are (a) 690 nm/300 nm, (b) 600 nm/300 nm, (c) 690 nm/510 nm, (d) 600 nm/590 nm, and (e) 600 nm/780 nm. Note that the microgels shrink to 35−50% of their initial size upon drying; therefore, their size in these images is smaller than that in solution.

the samples with microgel/latex ratios of 70 and 21, respectively.

As we show below, a latex particle of a given size binds (on average) a given number of microgels, which we will denote n. If the microgel/latex ratio in the dispersion is much larger than n, then each latex particle is surrounded by n microgels, and there is an excess of isolated microgels. As the microgel/latex ratio gets closer to n, latex particles may coordinate to microgels that are already bound to other latex particles and thereby form aggregates. When the microgel/latex ratio becomes smaller than n, there are not enough microgels in the solution to coat all latex particles, and thus, the aggregates grow to macroscopic dimensions and precipitate. The positive and negative microparticles do not behave symmetrically; that is, we never observed core−satellite assemblies comprising a microgel core and latex satellites. We attribute this asymmetry between positive and negative microparticles to the fact that the van der Waals (vdW) interactions between microgels are much weaker than those between latex particles (see the estimation of the vdW interaction strength in the Supporting Information). We expect, therefore, that latex-coated microgel particles will be much more prone to aggregation induced by vdW forces than the microgel-coated latex.

We consider now the factors that determine the number of microgel satellites per latex central particle (n) in mixtures where the microgel/latex ratio $\geq n$. Figure 2 clearly shows that the coordination number depends on the size of the microgel and the latex particles. Microgels are soft, charged particles, and therefore, they do not have a well-defined size (like a neutral hard sphere). We will consider, therefore, an effective size that we determined from the interparticle distance in two-dimensional hexagonal assemblies of microgels obtained by drop-casting (see the Supporting Information). This estimation of the size of the microgels includes electrostatic and polymer-mediated repulsive interactions and, therefore, is more reliable than that by dynamic light scattering (although, in practice, the sizes estimated by these two methods are similar; see Table 1). The coordination number can be either thermodynamically or kinetically controlled. In the case of thermodynamic control, microgels can reorganize on the surface of the latex in order to maximize the number of favorable latex−microgel electrostatic bonds and minimize repulsive microgel−microgel interactions. For example, the assembly of core−satellite particles with poly(vinylpyridine) latex cores and silica satellites is thermodynamically controlled as the silica satellites can easily transfer from one core particle to another.[33] We expect that in the presence of a large excess of microgels, thermodynamic control will maximize the number of microgel particles on the surface of the latex particle with the constraint that the distance between microgels should be smaller than their effective size. In contrast, under conditions of kinetic control, microgels randomly collide in solution with the assemblies and adsorb if they can reach the surface of the latex particle before colliding with a previously adsorbed microgel. Microgels cannot reorganize once they adsorb onto the latex particle; hence, adsorption ceases when the largest free site on the latex surface is smaller than the effective size of the microgel. This process is known as random sequential adsorption (RSA).[34−36] Examples of such a process are the adsorption of positively charged latex NPs on negatively charged latex microparticles[22,37] and the adsorption of NPs and dendrimers on oppositely charged surfaces.[35,36]

In order to determine whether the formation of latex−microgel core−satellite particles is kinetically or thermodynamically controlled, we determined the number of satellites per central particle n in our experiments as a function of the ratio of the sizes of the satellite and core particles, d_{sat}/d_{core}. We considered only isolated core−satellite assemblies in this analysis and corrected the value of n determined experimentally in order to account for the number of microgels that are hidden behind the latex core and, therefore, cannot be observed in a top-view SEM image (this correction was <10% for all combinations of latex and microgel particles under study; see the Supporting Information). In Figure 3, we show that the experimentally determined coordination numbers for different combinations of microgel and latex sizes are in much better agreement with the coordination numbers predicted for RSA than with those predicted for the maximum coordination resulting from thermodynamic control.

In a given sample, core particles are coated with different numbers of satellites, which gives rise to a distribution of the number of satellites per core (the vertical error bars in Figure 3 show one standard deviation from the average value). This

dx.doi.org/10.1021/jz5013609 | J. Phys. Chem. Lett. 2014, 5, 2775−2780

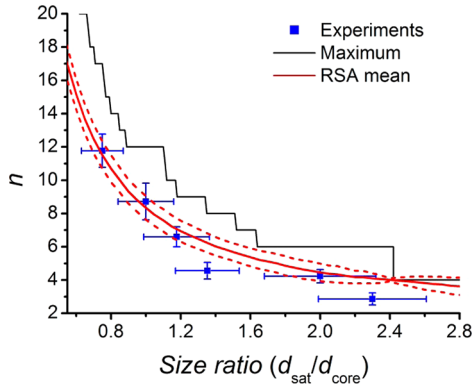

Figure 3. Coordination numbers (number of microgel particles per latex particle) as a function of the ratio of the diameter of the microgels (d_{sat}) and the latex particle (d_{core}) determined experimentally (points) and predicted for thermodynamic (black) and kinetic (red) control. The solid red line shows the mean value determined for RSA simulations, and the dashed red lines show the mean for RSA plus and minus the standard deviation. The results in this plot are also shown in Table S4 in the Supporting Information.

observation agrees with the RSA mechanism, where the number of satellites per central particle is determined by a series of random collisions and, therefore, has some intrinsic distribution (the dashed red lines in Figure 3 show the standard deviation of n predicted by the RSA model). The experimental width of the distribution decreases for increasing size ratio, $d_{sat}/d_{core,}$ and it is relatively small for samples with $d_{sat}/d_{core} = 2 (n = 4.2 \pm 0.4)$ and $d_{sat}/d_{core} = 2.3 (n = 2.9 \pm 0.4)$. Interestingly, the RSA process predicts that for $d_{sat}/d_{core} \approx 2.41$, all clusters have $n = 4$. This effect has been observed previously by Shade et al.[22]

We attribute the small quantitative discrepancies between our experimental results and the predictions of the RSA in Figure 3 to the underestimation of the size of the microgels in solution. This underestimation may arise from the one or more of the following factors: (i) Packing of microgels on planar substrates (which we used to estimate microgel size) is a complex process that is believed to occur at the air/water/substrate interface,[23−25] while assembly of core−satellite particles occurs in bulk solution. (ii) The RSA model used here assumes that the satellite particles are spheres with an effective diameter d_{sat}; however, microgels are soft particles and deform upon adsorption on the latex particle. This deformation is observed in SEM images of the assemblies after we dissolve the latex particles with toluene; see Figure S5 in the Supporting Information. Besides the quantitative differences observed in Figure 3, our experimental results and the RSA model also disagree in that we observe well-defined planar triangle and planar square structures in Figure 2a and b, respectively, but the RSA process produces random geometries rather than well-defined planar structures. We believe that our observation of planar structures is an artifact of the imaging process, that is, nonplanar solution-phase structures deform during adsorption onto the silicon substrate or during the drying process.[38]

The microgels and latex retain their positive and negative charges within the assembly. Figure 4a shows a color map of the electrostatic potential calculated for a core−satellite particle with a 510 nm central core and five 690 nm microgel particles (see details of the calculation in the Supporting Information). The figure shows that the microgel particles expose positively charged surfaces and the latex particles expose negatively charged surfaces. The calculations in Figure 4a were performed

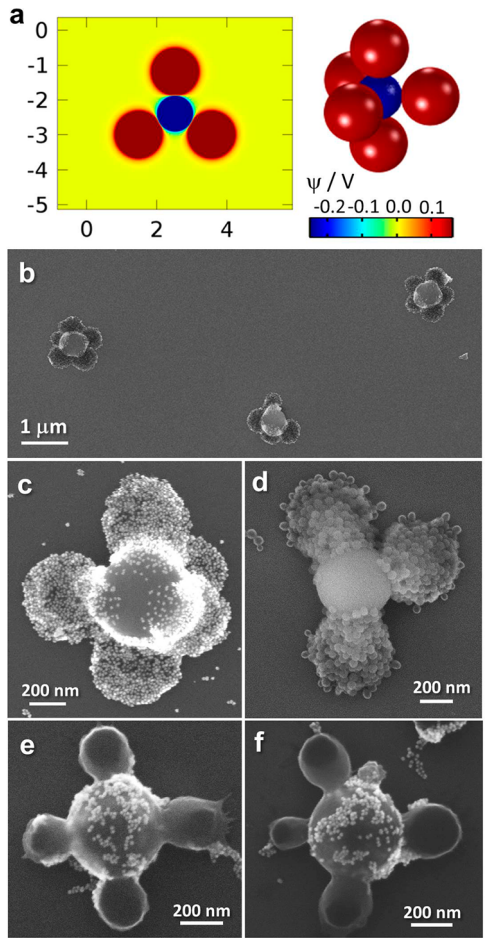

Figure 4. (a) Calculated electrostatic potential in a core−satellite particle composed of five 690 nm microgels adsorbed on a 510 nm latex particle (see the three-dimensional structure on the right) for an ionic strength of 10 μM. The electrostatic potential is plotted as a color map for a cross section defined by the centers of the three equatorial satellites (see details of the calculation in the Supporting Information). (b−f) SEM images of assemblies of negatively charged Au NPs (b,c), negatively charged polystyrene latex NPs (d), and positively charged Au NPs (e,f) on the latex−microgel core−satellite particles. The sizes of the microgels (in solution) and the latex particles are 690 and 510 nm, respectively (same sizes as in panel c of Figure 2).

for $I = 10$ μM (which is the minimum ionic strength of our solutions), but well-defined negative and positive charged regions exists for higher ionic strengths as well (see the Supporting Information). These charged regions can be used to adsorb small charged NPs to create hierarchical assemblies. Figure 4b−d shows latex−microgel−Au NP and latex−microgel−latex NP colloids, where negatively charged particles have adsorbed onto the positively charged microgels. It is important to stress that if these assemblies were formed under thermodynamic control, the addition of a large excess of small negatively charged NPs would disassemble the core−satellite NPs in order to produce NP-coated microgels. We observe, however, that the core−satellite structures are stable in the presence of the NPs, which agrees with our finding that latex−microgel particles are kinetically trapped structures. Figure 4e,f shows latex−microgel−Au NP assemblies where positively charged Au NPs have adsorbed onto the negatively charged latex cores.

dx.doi.org/10.1021/jz5013609 | J. Phys. Chem. Lett. 2014, 5, 2775−2780

In summary, we have demonstrated the preparation of core−satellite particles with latex cores and microgel satellites. A key result of our work is that the formation of core−satellite particles follows the RSA model and therefore is kinetically controlled. The latex−microgel electrostatic bonds are strong enough to prevent reorganization of the microgel satellites during assembly and dissociation of the latex−microgel structures in the presence of smaller charged NPs, a property that enables the formation of hierarchical structures. The bonds between components of the assembly are, however, labile enough to allow distortion of nonplanar solution-phase structures into planar structures on a substrate upon drying. In high salt environments or during purification, the electrostatic bonds between particles may dissociate, and thus, it might be necessary to stabilize our electrostatically assembled particles by chemical cross-linking.

The assembly of core−satellite structures by electrostatic interactions via the RSA mechanism is simple and potentially general as most microparticles and NPs are charged in water. It has, however, a number of limitations: (i) free satellite particles and/or large aggregates are always present in the dispersions of assemblies, (ii) there is a distribution of the number of satellites per central particle, and (iii) the assemblies do not have regular geometries. Future work will develop separation and purification methods in order to isolate assemblies of well-defined stoichiometry from an excess of satellite particles, large aggregates, and core−satellite particles with other stoichiometries. Note that our assembly method allows us to control the type of impurity in the system (isolated satellites or large aggregates) by adjusting the microgel/latex ratio but does not allow us to prepare pure assemblies. Due to the density contrast between the microgels (1.0−1.02 $g{\cdot}cm^{-3}$) and the central polystyrene latex (0.92−0.96 $g{\cdot}cm^{-3}$), density-based purification methods, such as analytical ultracentrifugation or magnetic levitation,[39] will be useful to isolate core−satellite particles from single microgels. Control over the geometry of the assemblies is more difficult than control over stoichiometry, although we show that planar structures can be prepared by adsorption onto a substrate.

Microgels are interesting materials to use as satellite particles due to their ability to respond to thermal and pH stimuli,[40] trap and deliver drugs,[41] and support catalytic enzymes[42] and NPs.[43] We believe that after replacing the latex particles with magnetic, plasmonic, or excitonic core materials, our assembly strategy will enable the preparation of well-defined multiresponsive colloids.

■ ASSOCIATED CONTENT

Supporting Information

Detailed experimental methods, examples of low-magnification wide-area SEM images, estimation of van der Waals interactions between latex and microgels, determination of microgel sizes from two-dimensional hexagonal assemblies, calculation of the electrostatic potential in latex−microgel core−satellite structures, and estimation of the fraction of microgels that cannot be observed by SEM. This material is available free of charge via the Internet at http://pubs.acs.org.

■ AUTHOR INFORMATION

Corresponding Author

*E-mail: e-weiss@northwestern.edu.

Notes

The authors declare no competing financial interest.

■ ACKNOWLEDGMENTS

This material is based upon work supported as part of the NERC (Non-Equilibrium Research Center), an Energy Frontier Research Center funded by the U.S. Department of Energy, Office of Science, Office of Basic Energy Sciences under Award Number DE-SC0000989. This work made use of the EPIC and Keck-II facilities of the NUANCE Center at Northwestern University for microscopy studies. The NUANCE Center is supported by NSF-NSEC, NSF-MRSEC, the Keck Foundation, the State of Illinois, and Northwestern University. M.T. acknowledges useful discussions with Yan Lu about synthesis of microgels. The authors thank Resham Banga and Chad Mirkin for the use of the dynamic light scattering setup.

■ REFERENCES

(1) Duguet, E.; Désert, A.; Perro, A.; Ravaine, S. Design and Elaboration of Colloidal Molecules: An Overview. *Chem. Soc. Rev.* **2011**, *40*, 941−960.

(2) Pawar, A. B.; Kretzschmar, I. Fabrication, Assembly, and Application of Patchy Particles. *Macromol. Rapid Commun.* **2010**, *31*, 150−168.

(3) Chen, Q.; Bae, S. C.; Granick, S. Directed Self-Assembly of a Colloidal Kagome Lattice. *Nature* **2011**, *469*, 381−384.

(4) van Blaaderen, A. Colloidal Molecules and Beyond. *Science* **2003**, *301*, 470−471.

(5) Wang, Y.; Wang, Y.; Breed, D. R.; Manoharan, V. N.; Feng, L.; Hollingsworth, A. D.; Weck, M.; Pine, D. J. Colloids with Valence and Specific Directional Bonding. *Nature* **2012**, *491*, 51−55.

(6) Hoffmann, M.; Wagner, C. S.; Harnau, L.; Wittemann, A. 3D Brownian Diffusion of Submicron-Sized Particle Clusters. *ACS Nano* **2009**, *3*, 3326−3334.

(7) Tikhomirov, G.; Hoogland, S.; Lee, P. E.; Fischer, A.; Sargent, E. H.; Kelley, S. O. DNA-Based Programming of Quantum Dot Valency, Self-Assembly and Luminescence. *Nat. Nano* **2011**, *6*, 485−490.

(8) Gellner, M.; Steinigeweg, D.; Ichilmann, S.; Salehi, M.; Schuetz, M.; Koempe, K.; Haase, M.; Schluecker, S. 3D Self-Assembled Plasmonic Superstructures of Gold Nanospheres: Synthesis and Characterization at the Single-Particle Level. *Small* **2011**, *7*, 3445−3451.

(9) Yoon, J. H.; Yoon, S. Probing Interfacial Interactions Using Core−Satellite Plasmon Rulers. *Langmuir* **2013**, *29*, 14772−14778.

(10) Lee, J.; Govorov, A. O.; Kotov, N. A. Nanoparticle Assemblies with Molecular Springs: A Nanoscale Thermometer. *Angew. Chem.* **2005**, *117*, 7605−7608.

(11) Gandra, N.; Abbas, A.; Tian, L.; Singamaneni, S. Plasmonic Planet−Satellite Analogues: Hierarchical Self-Assembly of Gold Nanostructures. *Nano Lett.* **2012**, *12*, 2645−2651.

(12) Ming, W.; Wu, D.; van Benthem, R.; de With, G. Superhydrophobic Films from Raspberry-Like Particles. *Nano Lett.* **2005**, *5*, 2298−2301.

(13) Tsai, H.-J.; Lee, Y.-L. Facile Method to Fabricate Raspberry-Like Particulate Films for Superhydrophobic Surfaces. *Langmuir* **2007**, *23*, 12687−12692.

(14) Snyder, C. E.; Ong, M.; Velegol, D. In-Solution Assembly of Colloidal Water. *Soft Matter* **2009**, *5*, 1263−1268.

(15) Sacanna, S.; Irvine, W. T. M.; Chaikin, P. M.; Pine, D. J. Lock and Key Colloids. *Nature* **2010**, *464*, 575−578.

(16) Kraft, D. J.; Vlug, W. S.; van Kats, C. M.; van Blaaderen, A.; Imhof, A.; Kegel, W. K. Self-Assembly of Colloids with Liquid Protrusions. *J. Am. Chem. Soc.* **2008**, *131*, 1182−1186.

(17) Xu, X.; Rosi, N. L.; Wang, Y.; Huo, F.; Mirkin, C. A. Asymmetric Functionalization of Gold Nanoparticles with Oligonucleotides. *J. Am. Chem. Soc.* **2006**, *128*, 9286−9287.

(18) Li, R.; Yang, X.; Li, G.; Li, S.; Huang, W. Core−Corona Polymer Composite Particles by Self-Assembled Heterocoagulation Based on a Hydrogen-Bonding Interaction. *Langmuir* **2006**, *22*, 8127−8133.
(19) Dey, P.; Zhu, S.; Thurecht, K. J.; Fredericks, P. M.; Blakey, I. Self Assembly of Plasmonic Core−Satellite Nano-assemblies Mediated by Hyperbranched Polymer Linkers. *J. Mater. Chem. B* **2014**, *2*, 2827−2837.
(20) Walker, D. A.; Kowalczyk, B.; de la Cruz, M. O.; Grzybowski, B. A. Electrostatics at the Nanoscale. *Nanoscale* **2011**, *3*, 1316−1344.
(21) Tagliazucchi, M.; Weiss, E. A.; Szleifer, I. Dissipative Self-Assembly of Particles Interacting through Time-Oscillatory Potentials. *Proc. Natl. Acad. Sci. U.S.A.* **2014**, *111*, 9751−9756.
(22) Schade, N. B.; Holmes-Cerfon, M. C.; Chen, E. R.; Aronzon, D.; Collins, J. W.; Fan, J. A.; Capasso, F.; Manoharan, V. N. Tetrahedral Colloidal Clusters from Random Parking of Bidisperse Spheres. *Phys. Rev. Lett.* **2013**, *110*, 148303.
(23) Tsuji, S.; Kawaguchi, H. Self-Assembly of Poly(*N*-isopropylacrylamide)-Carrying Microspheres into Two-Dimensional Colloidal Arrays. *Langmuir* **2005**, *21*, 2434−2437.
(24) Lu, Y.; Drechsler, M. Charge-Induced Self-Assembly of 2-Dimensional Thermosensitive Microgel Particle Patterns. *Langmuir* **2009**, *25*, 13100−13105.
(25) Horigome, K.; Suzuki, D. Drying Mechanism of Poly(*N*-isopropylacrylamide) Microgel Dispersions. *Langmuir* **2012**, *28*, 12962−12970.
(26) Gaulding, J. C.; Saxena, S.; Montanari, D. E.; Lyon, L. A. Packed Colloidal Phases Mediate the Synthesis of Raspberry-Structured Microgel Heteroaggregates. *ACS Macro Lett.* **2013**, *2*, 337−340.
(27) Suzuki, D.; Horigome, K. Assembly of Oppositely Charged Microgels at the Air/Water Interface. *J. Phys. Chem. B* **2013**, *117*, 9073−9082.
(28) Suzuki, D.; Horigome, K. Binary Mixtures of Cationic and Anionic Microgels. *Langmuir* **2011**, *27*, 12368−12374.
(29) Crassous, J. J.; Millard, P. E.; Mihut, A. M.; Polzer, F.; Ballauff, M.; Schurtenberger, P. Asymmetric Self-Assembly of Oppositely Charged Composite Microgels and Gold Nanoparticles (Vol. 8, pg 1648, 2012). *Soft Matter* **2012**, *8*, 12133−12133.
(30) McParlane, J.; Dupin, D.; Saunders, J. M.; Lally, S.; Armes, S. P.; Saunders, B. R. Dual pH-Triggered Physical Gels Prepared from Mixed Dispersions of Oppositely Charged pH-Responsive Microgels. *Soft Matter* **2012**, *8*, 6239−6247.
(31) Hou, Y.; Ye, J.; Wei, X. L.; Zhang, G. Z. Effects of Cations on the Sorting of Oppositely Charged Microgels. *J. Phys. Chem. B* **2009**, *113*, 7457−7461.
(32) Snoswell, D. R. E.; Rogers, T. J.; Howe, A. M.; Vincent, B. Controlling Porosity within Colloidal Heteroaggregates. *Langmuir* **2005**, *21*, 11439−11445.
(33) Balmer, J. A.; Mykhaylyk, O. O.; Fairclough, J. P. A.; Ryan, A. J.; Armes, S. P.; Murray, M. W.; Murray, K. A.; Williams, N. S. J. Unexpected Facile Redistribution of Adsorbed Silica Nanoparticles between Latexes. *J. Am. Chem. Soc.* **2010**, *132*, 2166−2168.
(34) Adamczyk, Z.; Belouschek, P. Localized Adsorption of Particles on Spherical and Cylindircal Interfaces. *J. Colloid Interface Sci.* **1991**, *146*, 123−136.
(35) Semmler, M.; Mann, E. K.; Rička, J.; Borkovec, M. Diffusional Deposition of Charged Latex Particles on Water−Solid Interfaces at Low Ionic Strength. *Langmuir* **1998**, *14*, 5127−5132.
(36) Pericet-Camara, R.; Papastavrou, G.; Borkovec, M. Atomic Force Microscopy Study of the Adsorption and Electrostatic Self-Organization of Poly(amidoamine) Dendrimers on Mica. *Langmuir* **2004**, *20*, 3264−3270.
(37) Sadowska, M.; Adamczyk, Z.; Nattich-Rak, M. Mechanism of Nanoparticle Deposition on Polystyrene Latex Particles. *Langmuir* **2014**, *30*, 692−699.
(38) Perro, A.; Nguyen, D.; Ravaine, S.; Bourgeat-Lami, E.; Lambert, O.; Taveau, J. C.; Duguet, E. Planar Submicronic Silica−Polystyrene Particles Obtained by Substrate-Directed Shaping. *J. Mater. Chem.* **2009**, *19*, 4225−4230.
(39) Mirica, K. A.; Shevkoplyas, S. S.; Phillips, S. T.; Gupta, M.; Whitesides, G. M. Measuring Densities of Solids and Liquids Using Magnetic Levitation: Fundamentals. *J. Am. Chem. Soc.* **2009**, *131*, 10049−10058.
(40) Lyon, L. A.; Serpe, M. J. *Hydrogel Micro and Nanoparticles*; John Wiley & Sons: New York, 2012.
(41) Oh, J. K.; Drumright, R.; Siegwart, D. J.; Matyjaszewski, K. The Development of Microgels/Nanogels for Drug Delivery Applications. *Prog. Polym. Sci.* **2008**, *33*, 448−477.
(42) Welsch, N.; Becker, A. L.; Dzubiella, J.; Ballauff, M. Core−Shell Microgels as "Smart" Carriers for Enzymes. *Soft Matter* **2012**, *8*, 1428−1436.
(43) Schrinner, M.; Ballauff, M.; Talmon, Y.; Kauffmann, Y.; Thun, J.; Moeller, M.; Breu, J. Single Nanocrystals of Platinum Prepared by Partial Dissolution of Au−Pt Nanoalloys. *Science* **2009**, *323*, 617−620.